Organic & Biomolecular Chemistry

ROYAL SOCIETY OF CHEMISTRY

PAPER

View Article Online
View Journal | View Issue

Cite this: *Org. Biomol. Chem.*, 2023, **21**, 6969

Balancing ring and stopper group size to control the stability of doubly threaded [3]rotaxanes†

Jerald E. Hertzog, [a,b] Guancen Liu, [a] Benjamin W. Rawe, [b] Vincent J. Maddi, [a] Laura F. Hart, [b] Jongwon Oh, [b] Neil D. Dolinski [b] and Stuart J. Rowan *[a,b,c]

Synthesizing doubly threaded [3]rotaxanes requires the use of larger rings than more traditional singly threaded [2]rotaxanes. A key challenge in accessing stable doubly threaded [3]rotaxanes with large rings is finding the right combination of ring to stopper size. In this study, a series of doubly threaded [3]rotaxanes derived from five different sized macrocycles in the size range of 40–48 atoms and two different stopper groups, which contain 1 or 2 tris(*p*-*t*-butylbiphenyl)methyl moieties, were prepared and their kinetic stability examined. These interlocked compounds were synthesized using a metal-templated approach and fully characterized utilizing a combination of mass spectrometry, NMR spectroscopy, and size-exclusion chromatography techniques. The effect of ring size on the stability of the doubly threaded [3]rotaxane was investigated *via* kinetic stability tests monitored using ^{1}H-NMR spectroscopy. By tightening the macrocycle systematically every 2 atoms from 48 to 40 atoms, a wide range of doubly threaded interlocked molecules could be accessed in which the rate of room temperature slippage of the macrocycle from the dumbbells could be tuned. Using the larger stopper group with a 48-atom ring results in no observable rotaxane, 46–44 atom macrocycles result in metastable rotaxane species with a slippage half-life of ~5 weeks and ~9 weeks, respectively, while macrocycles of 42 atoms or smaller yield a stable rotaxane. The smaller sized stopper is not able to fully stabilize any of the [3]rotaxane structures but metastable [3]rotaxanes are obtained with slippage half-lives of 25 ± 2 hours and 13 ± 1 days using macrocycles with 42 or 40 atoms, respectively. These results highlight the dramatic effect that relatively small ring size changes can have on the structure of doubly threaded [3]rotaxanes and lay the synthetic groundwork for a range of higher order doubly threaded interlocked architectures.

Received 13th July 2023,
Accepted 9th August 2023

DOI: 10.1039/d3ob01123b

rsc.li/obc

Introduction

Mechanically interlocked molecules (MIMs) are compounds comprised of multiple components that are connected as a result of their topology as opposed to a standard covalent bond.[1] This unusual connectivity has been exploited by scientists over the past few decades resulting in the exploration of MIMs in a wide range of applications including catalysis,[2,3] drug and gene delivery,[4,5] switchable surfaces,[6,7] mechanophores,[8–10] molecular machines[11,12] and more.[13,14] Specifically, their use as molecular machines received international acclaim with the awarding of the 2016 Nobel Prize in Chemistry to Sauvage,[15] Feringa,[16] and Stoddart.[17] A key aspect of MIMs for many such applications is how the individual components interact and are able to move relative to one another.[18]

Rotaxanes are a class of MIMs comprised of ring and dumbbell components.[19] The most elementary version is a singly threaded [2]rotaxane comprised of one macrocycle component kinetically trapped between the stopper groups of a second dumbbell component.[20] Matching the correctly sized ring to stopper group is critical for achieving a stable interlocked molecule,[21,22] and prior studies have shown that depending on the relative size of stopper and macrocycle, the ring may undergo a slippage process where it dethreads from the dumbbell yielding the noninterlocked components.[23–26] Accessing different slippage rates in these metastable rotaxanes is possible and such interlocked compounds have been shown to be useful as a means of chemical protection,[27,28] constructing molecular pumps,[29–31] and the assembly of more complex

[a]*Department of Chemistry, University of Chicago, Chicago, IL, 60637, USA. E-mail: stuartrowan@uchicago.edu*
[b]*Pritzker School of Molecular Engineering, University of Chicago, Chicago, IL 60637, USA*
[c]*Chemical Science and Engineering Division and Center for Molecular Engineering, Argonne National Laboratory, Lemont, IL 60434, USA*

†Electronic supplementary information (ESI) available: Synthetic procedures, spectroscopic data for new compounds, full NMR spectra of rotaxanes, and kinetic dethreading experimental details. See DOI: **https://doi.org/10.1039/d3ob01123b**

architectures such as molecular containers[32] and supramolecular networks.[33]

An important design parameter that has emerged in rotaxane synthesis and application is macrocycle size.[34–43] Specifically, control over the size of the ring(s) employed in rotaxane structures has allowed researchers to influence their ring mobility,[35] impact their electrochemical properties,[38] access molecular shuttles,[39] develop means of programmable chemical protection[40] and more. In these studies, relatively small changes (1–2 atoms) in macrocycle size result in dramatic effects in the resulting rotaxane function. However, the above-mentioned studies into metastable [2]rotaxanes, highlight that careful design and chemical consideration must be given to both rotaxane components if the goal is to access a stable rotaxane that can perform a useful function.

The rotaxanes discussed above are all based on a simple singly threaded [2]rotaxane motif. As researchers continue to access more complex interlocked structures, there is a growing interest in looking towards higher order rotaxanes[44] such as multiply threaded[45] architectures in order to achieve more complicated function. Bundling multiple threads within the same macrocyclic cavity opens the door to the possibility of tuning their inter-thread interactions through means such as non-covalent interactions or proximity-induced covalent chemistries. However, to date, the synthesis of doubly threaded [3]rotaxanes remains a challenging task,[45] and the effect of macrocycle size variation on the rotaxane structure has been far less explored in doubly threaded systems.[46–48] Recently, the synthesis and characterization of a series of metastable doubly threaded [3]rotaxanes that vary in stopper group size with one of the largest macrocycles to date (46 atoms) was reported.[49] Using a metal-templated strategy,[50] a ditopic 2,6-bis(*N*-alkyl-benzimidazolyl)pyridine (Bip)[51] containing macrocycle was complexed to two linear Bip-containing thread components before being stoppered using Cu-catalyzed click chemistry. Changing the stopper group size through varying the number of tris(*p*-*t*-butylbiphenyl)methyl (*t*BBM) moieties (from 1 to 4 *t*BBM units) made it possible to tune the interlocked stability of the metastable [3]rotaxanes with a resultant half-life in deuterated chloroform from <1 min to *ca.* 6 months at room temperature. However, in these initial studies, a stable [3]rotaxane structure was not fully realized, highlighting the difficulty of fully stoppering such large rings.

The goal of this work was to examine the effect that both ring and stopper size has on the stability of these Bip-derived doubly threaded [3]rotaxanes. Specifically, four additional macrocycles in the size range of 40–48 atoms (Fig. 1a) were synthesized and, after metal-templated assembly with the linear Bip-containing thread (Fig. 1b), were tested for their ability to form doubly threaded [3]rotaxanes with two different sized stopper groups consisting of either one or two *t*BBM moieties (Fig. 1c).

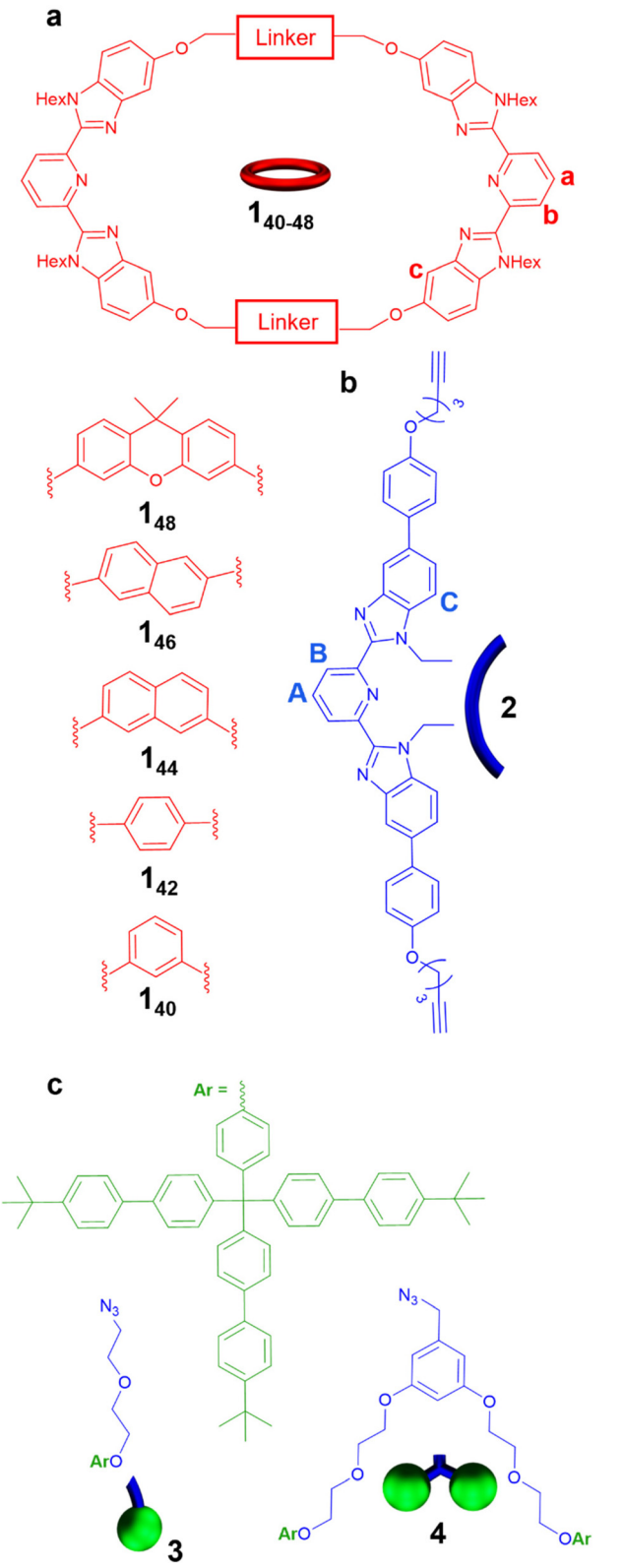

Fig. 1 Chemical structure of the (a) macrocycle components $\mathbf{1}_{40-48}$, (b) alkyne terminated thread component **2**, and (c) two differently sized azide functionalized stopper groups that have either one (**3**) or two (**4**) tris(*p*-*t*-butylbiphenyl)methyl (tBBM) moieties.

Results and discussion

The ditopic Bip-containing macrocycles $\mathbf{1_N}$ (where N = 40, 42, 44, 46, or 48 atoms, Fig. 1a) were synthesized and fully charac-

terized from their corresponding bis-phenolic Bip derivatives *via* Williamson ether synthesis (see ESI, Fig. S1–S4† for full synthetic details). The five rings all contain a different rigid aromatic linker resulting in the ability to systematically vary the ring size (defined here as the total number of atoms that comprise the inner circumference of the macrocycle[52,53]) by 2 atoms from 48 to 40. The bis-alkyne linear thread component **2** and azide-functionalized stopper groups **3** (with one tBMM moiety) and **4** (with two tBMM moieties) were synthesized according to previously published methods (Fig. 1b and c).[49]

With these components in hand, the first step towards attempting [3]rotaxane synthesis with these four new rings was to form a series of doubly threaded pseudo[3]rotaxanes with the thread component **2**. In order to do this, a metal-templated assembly process was used (Fig. 2a).[49] First 1 : 2 solutions of the appropriate ring components (**$1_{40–48}$**) with the thread component **2** were prepared and checked *via* ^{1}H-NMR spectroscopy to obtain the correct 1 : 2 stoichiometry. Then, 2 equivalents of $Fe(NTf_2)_2$ was titrated into each mixture of components followed by heating for 1 day at 45 °C to reach full equilibration and form the doubly threaded pseudo[3]rotaxanes **$1_{40–48}$:2_2**:Fe(II)$_2$. Each self-assembly reaction was monitored using ^{1}H-NMR spectroscopy. This revealed the appearance of new signals that are shifted from the unbound components, and based on previously published metal-templated Bip complexes[49,54,55] the diagnostic pyridyl peaks can be easily assigned (see ESI, Fig. S5–S12†). The obtained doubly-threaded pseudo[3]rotaxanes **$1_{40–48}$:2_2**:Fe(II)$_2$ in each case is a result of the principle of maximal site occupancy,[56] the rigidity present in the ring components, and the exact stoichiometry used.

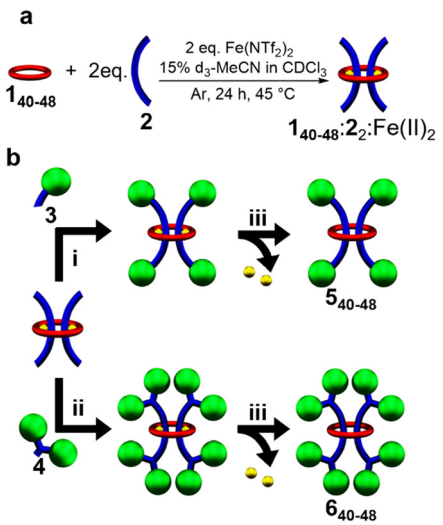

Fig. 2 (a) Scheme showing assembly of doubly threaded pseudo[3]rotaxanes **$1_{40–48}$:2_2**:Fe(II)$_2$. (b) Stoppering with component **3** followed by demetallation to access the series of doubly threaded [3]rotaxanes **$5_{40–48}$** (top) and stoppering with component **4** followed by demetallation to access the series of doubly threaded [3]rotaxanes **$6_{40–48}$** (bottom). Reaction conditions: (i) 6 eq. **3**, 10 eq. NaAsc, 1eq. Cu$(SO_4)\cdot 5H_2O$, DCM/H_2O, 25 °C, 24 h (ii) 6 eq. **4**, 10 eq. NaAsc, 1 eq. Cu$(SO_4)\cdot 5H_2O$, DCM/H_2O, 25 °C, 24 h (iii) excess TBAOH, DCM/MeCN/MeOH, 15 min.

With the range of pseudo[3]rotaxanes in hand, efforts then turned to stoppering them with either of the two stoppers **3** and **4** (Fig. 2b). Stoppering **$1_{40–48}$:2_2**:Fe(II)$_2$ with **3** would allow access to the doubly threaded compounds **$5_{40–48}$** while the larger stopper group **4** was used to access the doubly threaded series **$6_{40–48}$** (Fig. 3). Copper-catalysed azide–alkyne cycloaddition[57,58] was employed as the stoppering chemistry in order to ensure efficient addition of the stopper group (see ESI, Fig. S13–S21† for full synthetic details including the synthesis of the free dumbbell components **7** (stoppered with **3**) and **8** (stoppered with **4**)). After the stoppering reaction was completed, demetallation of the iron templating agent from the Bip ligands was achieved using base. As **5_{46}** and **6_{46}** are both known to be metastable species,[49] (specifically $t_{1/2}$ **5_{46}** ≪ 1 min and **6_{46}** = 5 weeks at ambient conditions in $CDCl_3$) analyzing each [3]rotaxane as quickly as possible upon demetallation was critical. As such, each crude demetallated product was analysed immediately *via* ^{1}H-NMR spectroscopy and MALDI-TOF mass spectrometry.

In the attempt to synthesize **6_{48}**, only the free components **8** and **1_{48}** were obtained in the resulting crude reaction mixture, as confirmed by ^{1}H-NMR spectroscopy (Fig. 4a–b and see ESI Fig. S22†) which showed no upfield shifted signals that are diagnostic in prior interlocked Bip-based compounds.[49,59] In addition, only the free dumbbell and ring were detected using MALDI-TOF mass spectrometry (see ESI, Fig. S23†). Similarly, only the free components **7** and **1_{44}** were observed in the attempt to make **5_{44}** as no upfield shifted product was observed *via* ^{1}H-NMR spectroscopy and no peak corresponding to the [3]rotaxane was detected using MALDI-TOF mass spectrometry (Fig. 4a and c and see ESI Fig. S24–S25†). Taken together, these results imply the ring size of **1_{48}** (48 atoms) is too large for the stopper group **4** and the 44 atom ring is too big for the smaller stopper group **3** to successfully stabilize either [3]rotaxane on any appreciable timescale (Fig. 5a and b). These results set the upper ceiling of ring sizes for these two stoppering groups in this Bip-based doubly threaded [3]rotaxane system.

The analysis of the crude reaction mixtures of [3]rotaxanes **5_{40}**, **5_{42}**, **6_{40}**, **6_{42}**, and **6_{44}** provided a significantly different result. In all five cases, dominant upfield shifted signals relative to the corresponding noninterlocked components were observed *via* ^{1}H-NMR spectroscopy (Fig. 4 and see ESI Fig. S26–S30†). In all five cases the crude yield (based on ^{1}H-NMR) of the interlocked product averaged 83 ± 2%. The presence of these upfield shifted signals is consistent with the shielding effect seen from interlocking molecules derived from the Bip ligand.[49,59] Preparative thin layer chromatography was then used to isolate the lower R_f interlocked products in varying amounts (11.1 mg – 33.5 mg) and yields (70% for **6_{40}**, 73% for **6_{42}**, 75% for **6_{44}**, 42% for **5_{40}**, and 34% for **5_{42}**). MALDI-TOF mass spectrometry confirmed the expected isotopic distribution of the high molecular weight [3]rotaxane peak for each **5_{40}**, **5_{42}**, **6_{40}**, **6_{42}**, and **6_{44}** (see ESI, Fig. S31–S35†), as

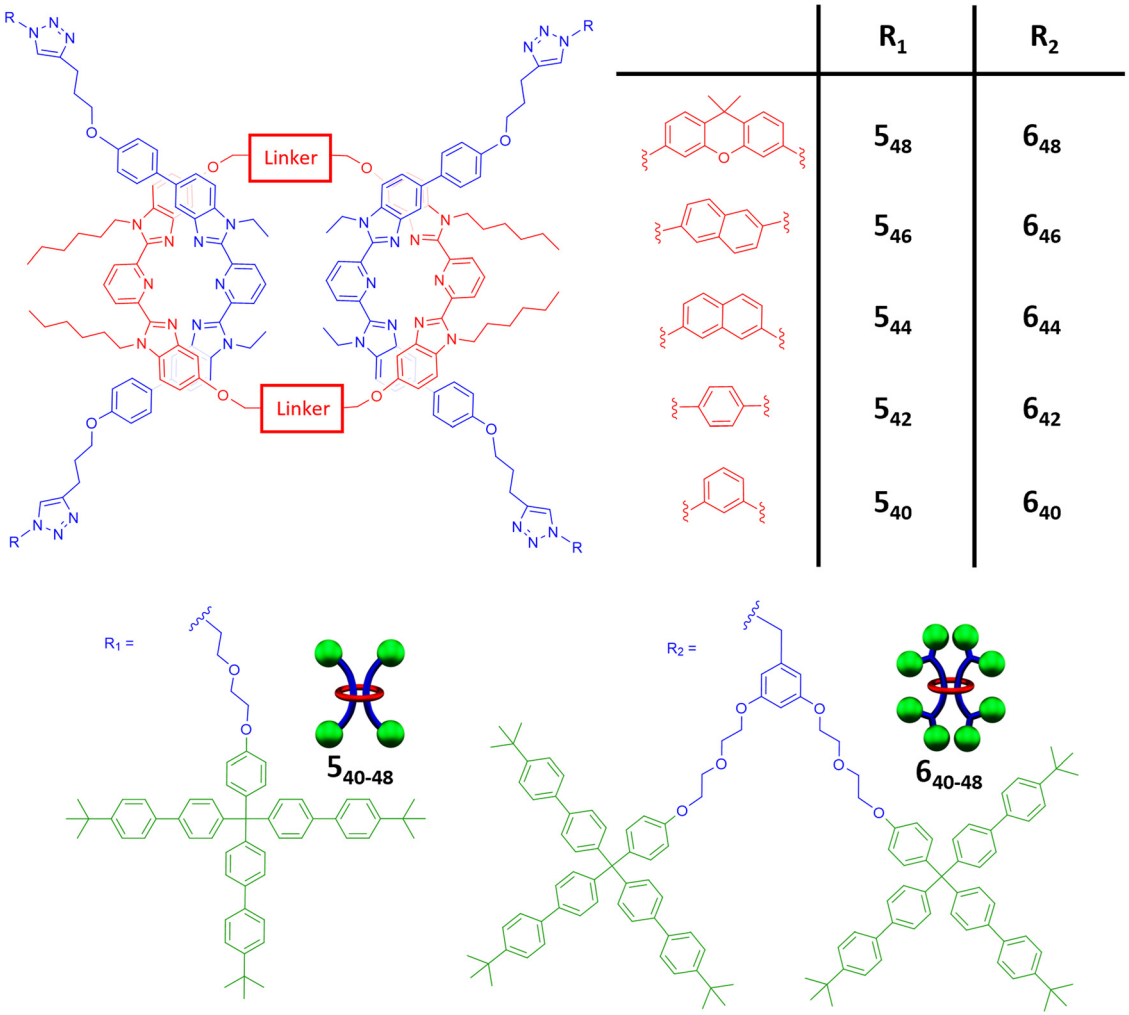

	R_1	R_2
	5_{48}	6_{48}
	5_{46}	6_{46}
	5_{44}	6_{44}
	5_{42}	6_{42}
	5_{40}	6_{40}

Fig. 3 Chemical structure of the doubly threaded [3]rotaxane series 5_{40-48} and 6_{40-48}.

well as the observed fragmentation pattern of the interlocked structure. In addition, GPC analysis revealed a lower retention time peak for 5_{40}, 5_{42}, 6_{40}, 6_{42}, and 6_{44} relative their corresponding noninterlocked components, consistent with the formation of the larger sized interlocked molecules (Fig. 6 and see ESI Fig. S36–S40†).

^{1}H-NMR analysis of the purified [3]rotaxanes 5_{40}, 5_{42}, 6_{40}, 6_{42}, and 6_{44} combined with ^{1}H–^{1}H COSY, comparison to each [3]rotaxane's noninterlocked components, and previously published NMR spectra[49] on 6_{46} allows the full ^{1}H-NMR spectra of 5_{40}, 5_{42}, 6_{40}, 6_{42}, and 6_{44} to be assigned (see ESI, Fig. S41–S50†). As noted, in all cases similar upfield shifting (relative to their noninterlocked components) of the component peaks is observed *via* ^{1}H-NMR spectroscopy upon formation of the [3]rotaxanes. However, there are some slight differences in the amount of upfield shifting. For instance, when comparing the ^{1}H-NMR spectra of 5_{40} and 6_{40} and their components, the larger stopper group in 6_{40} results in a slightly larger shift (0.18 ppm *vs.* 0.13 ppm) of the diagnostic aromatic peaks in 1_{40} (Fig. 7a and see ESI Fig. S51†), and a similar result is observed in the 42-atom system (5_{42} *vs.* 6_{42}, see ESI Fig. S51†). When comparing different ring sizes among compounds with the same stopper, the aromatic pyridinyl Bip resonances become particularly diagnostic with ring size in the 6_{40-46} series (labelled A and B in Fig. 7b). As the ring is tightened from 46 atoms in 6_{46} to 40 atoms in 6_{40} the pyridinyl resonances shift downfield incrementally, implying the pyridine ring in the dumbbell components spends less time close to the ring (Fig. 7b). To probe this 6_{40-46} [3]rotaxane series further, a full ^{1}H–^{1}H NOESY NMR analysis of each rotaxane and its corresponding noninterlocked control (2 : 1 solution of free dumbbell : macrocycle at same concentration) was conducted at the slightly reduced temperature of 278 K to enhance the NOE interactions. This analysis revealed a significant increase in the number of observable intercomponent NOEs (9 in 6_{46} increasing to 38 in 6_{40}) in the [3]rotaxanes upon ring tightening consistent with a closer proximity of the dumbbell components within the ring (see ESI, Fig. S52–S57†). Further examination of the specific NOE interactions that appear with ring size reduction reveal that the majority inter-

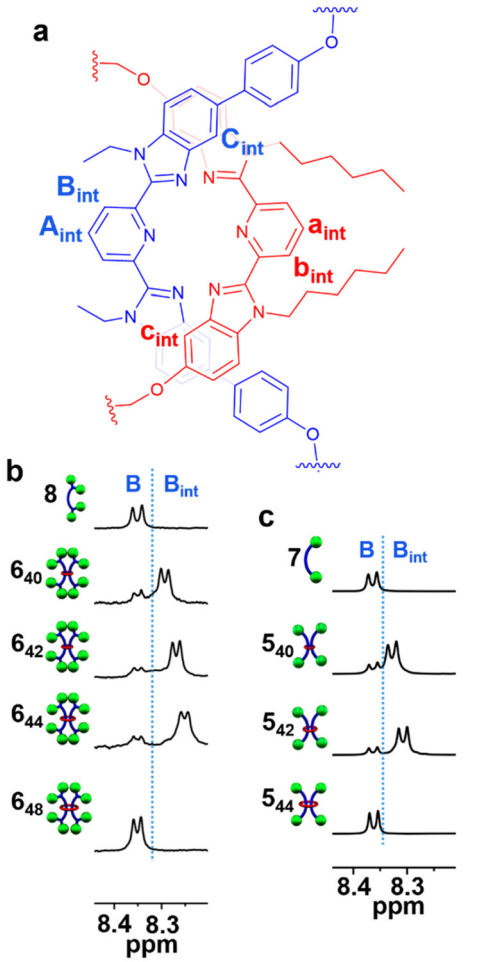

Fig. 4 (a) Selected ^{1}H NMR assignments for spectra. Partial crude ^{1}H-NMR overlay (500 MHz, $CDCl_3$, 25 °C) showing the region corresponding to the H_B peaks of (b) crude $\mathbf{6}_{40}$, $\mathbf{6}_{42}$, $\mathbf{6}_{44}$, the attempt to make $\mathbf{6}_{48}$, and the free dumbbell **8** for comparison, and (c) crude $\mathbf{5}_{40}$, $\mathbf{5}_{42}$, the attempt to make $\mathbf{5}_{44}$, and the free dumbbell **7** for comparison.

act with the dumbbell component near the middle pyridine ring of the dumbbell and the end diethylene glycol linker near the stopper group (see ESI, Fig. S58†) which is consistent with previously published all-atom molecular dynamics simulations of $\mathbf{6}_{46}$ that suggest an asymmetric orientation of the two dumbbells where the ring assumes a position near a stopper group of one dumbbell and in the middle of the other.[49]

As a result of the known metastability[49] of $\mathbf{6}_{46}$ and the observed instability of $\mathbf{6}_{48}$ and $\mathbf{5}_{44}$, investigating the kinetic stability of $\mathbf{5}_{40}$, $\mathbf{5}_{42}$, $\mathbf{6}_{40}$, $\mathbf{6}_{42}$, and $\mathbf{6}_{44}$ was of particular interest. As the most widely accepted definition of a rotaxane is that the interlocked structure must remain stable at ambient conditions,[60,61] a 3-week kinetic experiment at room temperature in deuterated chloroform was conducted. Freshly prepared solutions (1 mM **5** or **6**, $CDCl_3$) of $\mathbf{5}_{40}$, $\mathbf{5}_{42}$, $\mathbf{6}_{40}$, $\mathbf{6}_{42}$, and $\mathbf{6}_{44}$ were monitored twice a week at 25 °C *via* ^{1}H-NMR spectroscopy which allowed determination of stability for these interlocked molecules (Fig. 8).

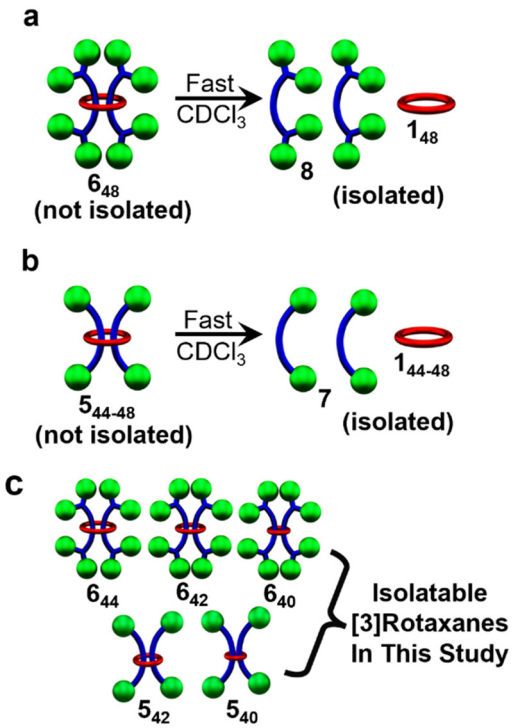

Fig. 5 Scheme depicting the observed rapid dethreading of (a) $\mathbf{6}_{48}$ and (b) $\mathbf{5}_{44-48}$ and (c) schematic representation of the isolatable [3]rotaxanes considered in this study.

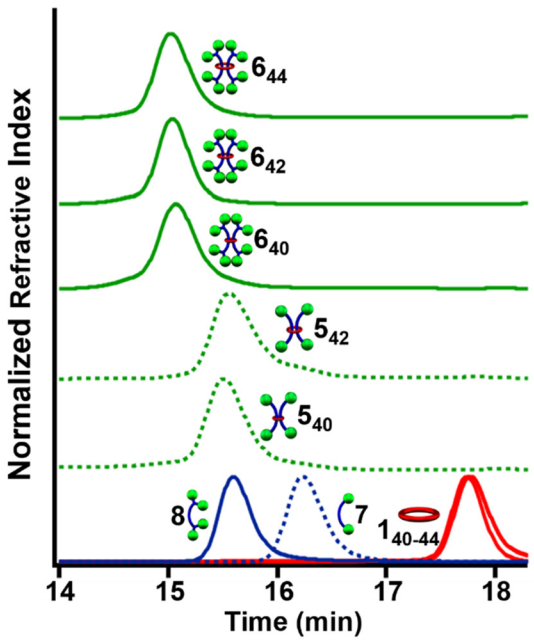

Fig. 6 GPC (eluent 3 : 1 THF : DMF) comparison of [3]rotaxanes $\mathbf{5}_{40}$, $\mathbf{5}_{42}$, $\mathbf{6}_{40}$, $\mathbf{6}_{42}$, and $\mathbf{6}_{44}$, dumbbell components **7** and **8**, and macrocycle components $\mathbf{1}_{40-44}$.

For $\mathbf{5}_{42}$, $\mathbf{5}_{40}$, and $\mathbf{6}_{44}$, the upfield shifted peaks assigned to interlocked product decreased during the experiment while the signals corresponding to the free noninterlocked com-

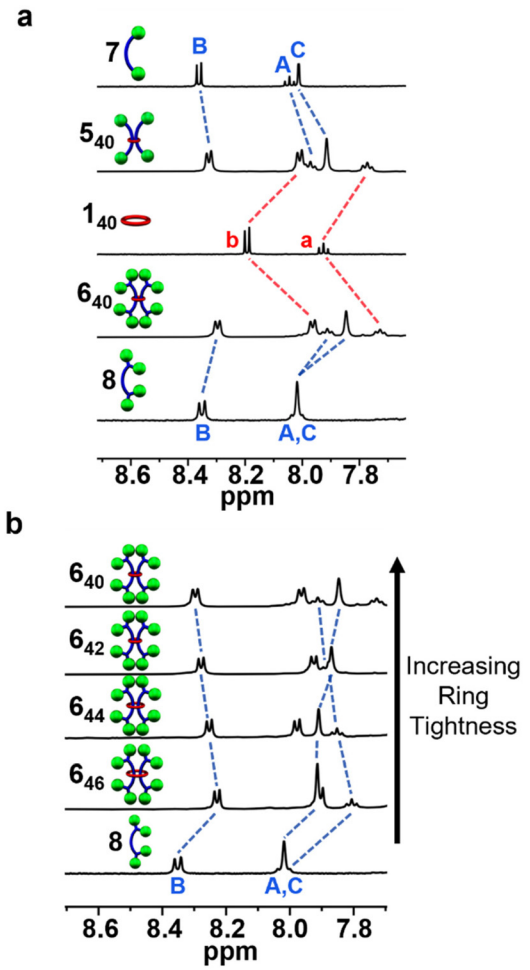

Fig. 7 Partial ^{1}H-NMR overlay (500 MHz, $CDCl_3$, 25 °C) of (a) [3]rotaxanes $\mathbf{5}_{40}$ and $\mathbf{6}_{40}$ and their free components $\mathbf{1}_{40}$, **7**, and **8** and (b) [3]rotaxanes $\mathbf{6}_{40-46}$ and dumbbell component **8** (labels correspond to Fig. 1).

ponents increased indicating that these [3]rotaxanes are metastable (Fig. 8a–c and see ESI, Fig. S59–S62†). No [2]rotaxane intermediates were observed in any of the slippage experiments suggesting the corresponding [2]rotaxanes ($\mathbf{5}_{42}$, $\mathbf{5}_{40}$, and $\mathbf{6}_{44}$) are not stable on any appreciable timescale. Kinetic analysis revealed that the observed slippage processes followed first-order kinetics dependent on the metastable [3]rotaxane concentration. Varying half-lives were obtained for the different interlocked compounds ranging from ~1 day to ~9 weeks highlighting the ability of component design to control the stability of the interlocked structure (Fig. 9 and see ESI Fig. S62† for full kinetic analysis).

$\mathbf{5}_{42}$ displayed the fastest observable slippage process as this [3]rotaxane rapidly fell apart to its noninterlocked components with a half-life of 25 ± 2 hours. In fact, $\mathbf{5}_{42}$ had to be kinetically analysed faster than the other [3]rotaxanes (once a day *vs.* biweekly) in order to obtain enough usable kinetic data for analysis (see ESI, Fig. S61†). $\mathbf{5}_{40}$ exhibited a significantly slower rate of slippage of 13 ± 1 days on account of the tighter fitting 40-atom ring. Even slower, the larger stoppered $\mathbf{6}_{44}$ slipped at a rate of 9 ± 1 weeks on a more similar timescale as the previously published $\mathbf{6}_{46}$ ($t_{1/2}$ = 5 weeks).[49] For $\mathbf{6}_{42}$ and $\mathbf{6}_{40}$, on the other hand, the upfield shifted peaks remained unchanged indicating that no slippage was observed (Fig. 8d–e and see ESI Fig. S63 and S64†) confirming these compounds are indeed stable doubly threaded [3]rotaxanes. The reduction from 44 atoms to 42 atoms in the ring component appears to be a critical point in this Bip-based [3]rotaxane series from a stability standpoint as this transition makes the [3]rotaxane **6** stable and **5** become isolatable. Given the fact that it is possible to access stable [3]rotaxanes ($\mathbf{6}_{42}$ and $\mathbf{6}_{40}$), metastable [3]rotaxanes ($\mathbf{5}_{40}$, $\mathbf{5}_{42}$, and $\mathbf{6}_{44}$), and species that are not observable on any reasonable timescale ($\mathbf{6}_{48}$ and $\mathbf{5}_{44-48}$), it can be seen that the entire kinetic window of stability can be accessed with

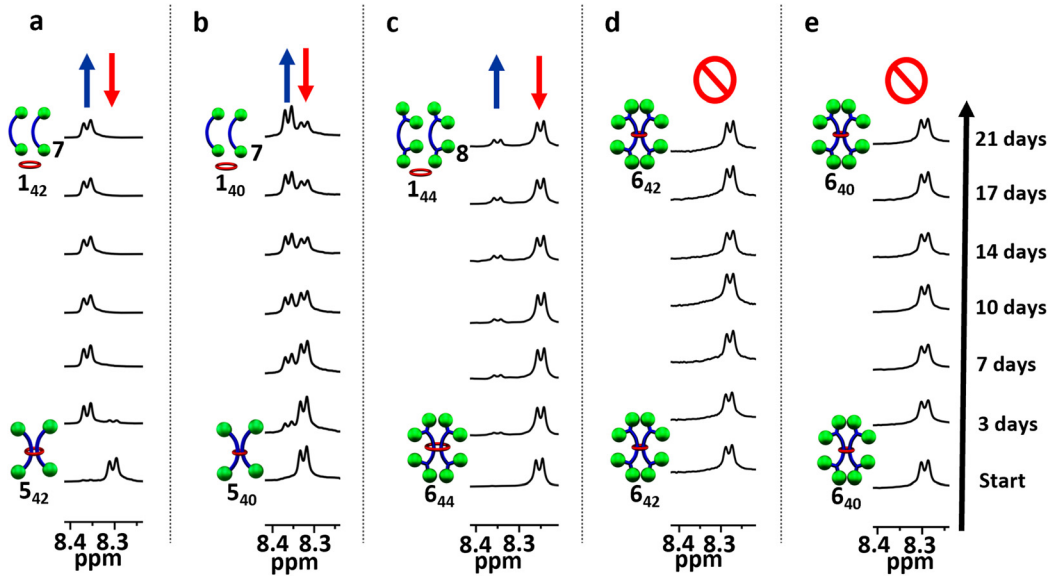

Fig. 8 Partial ^{1}H-NMR overlay (500 MHz, $CDCl_3$, 25 °C) of the 3-week slippage experiments of (a) $\mathbf{5}_{42}$, (b) $\mathbf{5}_{40}$, (c) $\mathbf{6}_{44}$, (d) $\mathbf{6}_{42}$, and (e) $\mathbf{6}_{40}$.

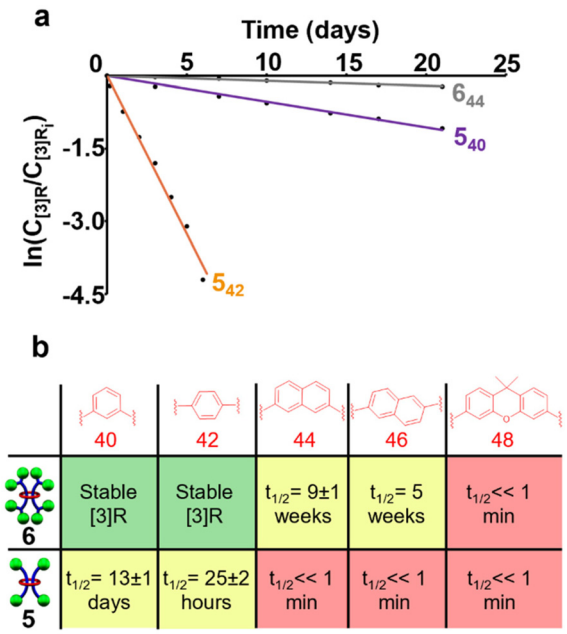

Fig. 9 (a) Kinetic first-order plot showing room temperature slippage of metastable [3]rotaxanes $\mathbf{5_{42}}$, $\mathbf{5_{40}}$, and $\mathbf{6_{44}}$ that were analysed in this study and (b) table summarizing kinetic half-lives of Bip-based doubly threaded [3]rotaxanes **5** and **6**.

this system. The stable [3]rotaxanes $\mathbf{6_{42}}$ and $\mathbf{6_{40}}$ described here are particularly exciting as they lay the synthetic groundwork for a range of doubly threaded polyrotaxane materials which have proven particularly challenging to access.[62–66]

Conclusions

In this study a series of doubly threaded [3]rotaxanes with two different sized stopper groups and five different rings in the size range of 40–48 atoms was considered. Kinetic stability tests revealed that the size of the ring had a profound effect on the [3]rotaxane stability. In particular, the entire kinetic stability window of these [3]rotaxanes, from not stable on any appreciable timescale to metastable to fully stable, could be observed by tightening the ring from 48 to 40 atoms using the larger stoppered system. The smaller stoppered system could not fully be stabilized at room temperature highlighting the difficulty of achieving a stable rotaxane with large rings. It is worthwhile pointing out that while the number of atoms is used here as a proxy for ring size other factors such as ring flexibility and conformation may also play a role in determining the stability of a rotaxane. Overall, the fully stable [3]rotaxanes described in this work open the door to an array of doubly threaded interlocked materials. The wide range of macrocycle size variation available in this system provides a versatile platform to investigate the effect of ring tightness on the sliding transition and unique interthread interactions available. This is currently being extended to the corresponding doubly-threaded polyrotaxane and slide-ring materials in our lab. For example, combining the optimized rotaxane component sizes determined in this work with synthetic procedures from slide-ring polycatenane networks[66] may provide one route to the little studied doubly threaded slide-ring networks.

Data availability

The authors declare that all data supporting the findings of this study are available within the article and ESI,† and raw data files are available from the corresponding author upon reasonable request.

Author contributions

JEH and SJR proposed the study. JEH conducted the synthesis and purification of all starting components and [3]rotaxanes with assistance from GL, BWR, LFH, JO and VJM. JEH conducted the ^{1}H-NMR, MALDI-TOF, and Size Exclusion Chromatography analysis of all materials described with assistance from GL and BWR. JEH, BWR, and NDD came up with the experimental design. SJR supervised the work. JEH, BWR, NDD, and SJR wrote the manuscript and made the figures. All authors discussed and commented on the manuscript.

Conflicts of interest

There are no conflicts to declare.

Acknowledgements

This work was funded by National Science Foundation (NSF) grant numbers CHE-1903603 and CHE-2304633. This work made use of the shared facilities at the University of Chicago Materials Research Science and Engineering Center (MRSEC), supported by National Science Foundation (NSF) under award number DMR-2011854. We would like to thank the University of Chicago Chemistry NMR Facility and the facility manager Dr Josh Kurutz for helpful discussion on NMR analysis. Parts of this work were carried out at the Soft Matter Characterization Facility (SMCF) of the University of Chicago. We would also like to thank the director of the SMCF, Dr Philip Griffin, for his assistance with GPC characterization.

References

1 J. F. Stoddart, The Chemistry of the Mechanical Bond, *Chem. Soc. Rev.*, 2009, **38**(6), 1802–1820, DOI: 10.1039/b819333a.
2 J. E. M. Lewis, M. Galli and S. M. Goldup, Properties and Emerging Applications of Mechanically Interlocked

Ligands, *Chem. Commun.*, 2017, **53**(2), 298–312, DOI: 10.1039/C6CC07377H.

3 E. M. G. Jamieson, F. Modicom and S. M. Goldup, Chirality in Rotaxanes and Catenanes, *Chem. Soc. Rev.*, 2018, **47**(14), 5266–5311, DOI: 10.1039/c8cs00097b.

4 K. K. Cotí, M. E. Belowich, M. Liong, M. W. Ambrogio, Y. A. Lau, H. A. Khatib, J. I. Zink, N. M. Khashab and J. F. Stoddart, Mechanised Nanoparticles for Drug Delivery, *Nanoscale*, 2009, **1**(1), 16–39, DOI: 10.1039/b9nr00162j.

5 A. Tamura and N. Yui, Threaded Macromolecules as a Versatile Framework for Biomaterials, *Chem. Commun.*, 2014, **50**(88), 13433–13446, DOI: 10.1039/C4CC03709J.

6 J. J. Davis, G. A. Orlowski, H. Rahman and P. D. Beer, Mechanically Interlocked and Switchable Molecules at Surfaces, *Chem. Commun.*, 2010, **46**(1), 54–63, DOI: 10.1039/b915122b.

7 T. Takata, Switchable Polymer Materials Controlled by Rotaxane Macromolecular Switches, *ACS Cent. Sci.*, 2020, **6**(2), 129–143, DOI: 10.1021/acscentsci.0c00002.

8 M. Zhang and G. De Bo, Mechanical Susceptibility of a Rotaxane, *J. Am. Chem. Soc.*, 2019, **141**(40), 15879–15883, DOI: 10.1021/jacs.9b06960.

9 M. Zhang and G. De Bo, A Catenane as a Mechanical Protecting Group, *J. Am. Chem. Soc.*, 2020, **142**(11), 5029–5033, DOI: 10.1021/jacs.0c01757.

10 T. Muramatsu, Y. Okado, H. Traeger, S. Schrettl, N. Tamaoki, C. Weder and Y. Sagara, Rotaxane-Based Dual Function Mechanophores Exhibiting Reversible and Irreversible Responses, *J. Am. Chem. Soc.*, 2021, **143**(26), 9884–9892, DOI: 10.1021/jacs.1c03790.

11 S. Erbas-Cakmak, D. A. Leigh, C. T. McTernan and A. L. Nussbaumer, Artificial Molecular Machines, *Chem. Rev.*, 2015, **115**(18), 10081–10206, DOI: 10.1021/acs.chemrev.5b00146.

12 C. J. Bruns and J. F. Stoddart, *The Nature of the Mechanical Bond: From Molecules to Machines*, Wiley, Hoboken, NJ, 2016. DOI: 10.1002/9781119044123.

13 S. F. M. Van Dongen, S. Cantekin, J. A. A. W. Elemans, A. E. Rowan and R. J. M. Nolte, Functional Interlocked Systems, *Chem. Soc. Rev.*, 2014, **43**(1), 99–122, DOI: 10.1039/c3cs60178a.

14 D. Sluysmans and J. F. Stoddart, The Burgeoning of Mechanically Interlocked Molecules in Chemistry, *Trends Chem.*, 2019, **1**(2), 185–197, DOI: 10.1016/j.trechm.2019.02.013.

15 J.-P. Sauvage, From Chemical Topology to Molecular Machines (Nobel Lecture), *Angew. Chem., Int. Ed.*, 2017, **56**(37), 11080–11093, DOI: 10.1002/anie.201702992.

16 B. L. Feringa, The Art of Building Small: From Molecular Switches to Motors (Nobel Lecture), *Angew. Chem., Int. Ed.*, 2017, **56**(37), 11060–11078, DOI: 10.1002/anie.201702979.

17 J. F. Stoddart, Mechanically Interlocked Molecules (MIMs)-Molecular Shuttles, Switches, and Machines (Nobel Lecture), *Angew. Chem., Int. Ed.*, 2017, **56**(37), 11094–11125, DOI: 10.1002/anie.201703216.

18 E. R. Kay, D. A. Leigh and F. Zerbetto, Synthetic Molecular Motors and Mechanical Machines, *Angew. Chem., Int. Ed.*, 2007, **46**(1–2), 72–191, DOI: 10.1002/anie.200504313.

19 I. T. Harrison and S. Harrison, Synthesis of a Stable Complex of a Macrocycle and a Threaded Chain, *J. Am. Chem. Soc.*, 1967, **89**(22), 5723–5724.

20 M. Xue, Y. Yang, X. Chi, X. Yan and F. Huang, Development of Pseudorotaxanes and Rotaxanes: From Synthesis to Stimuli-Responsive Motions to Applications, *Chem. Rev.*, 2015, **115**(15), 7398–7501, DOI: 10.1021/cr5005869.

21 F. M. Raymo, K. N. Houk and J. F. Stoddart, The Mechanism of the Slippage Approach to Rotaxanes, Origin of the "All-or-Nothing" Substituent Effect, *J. Am. Chem. Soc.*, 1998, **120**(36), 9318–9322, DOI: 10.1021/ja9806229.

22 M. Asakawa, P. R. Ashton, R. Ballardini, V. Balzani, M. Bělohradský, M. T. Gandolfi, O. Kocian, L. Prodi, F. M. Raymo, J. F. Stoddart and M. Venturi, The Slipping Approach to Self-Assembling [n]Rotaxanes, *J. Am. Chem. Soc.*, 1997, **119**(2), 302–310, DOI: 10.1021/ja961817o.

23 C. Heim, A. Affeld, M. Nieger and F. Vögtle, Size Complementarity of Macrocyclic Cavities and Stoppers in Amide-Rotaxanes, *Helv. Chim. Acta*, 1999, **82**(5), 746–759, DOI: 10.1002/(SICI)1522-2675(19990505)82:5<746::AID-HLCA746>3.0.CO;2-C.

24 J. Groppi, L. Casimiro, M. Canton, S. Corra, M. Jafari-Nasab, G. Tabacchi, L. Cavallo, M. Baroncini, S. Silvi, E. Fois and A. Credi, Precision Molecular Threading/Dethreading, *Angew. Chem., Int. Ed.*, 2020, **59**(35), 14825–14834, DOI: 10.1002/anie.202003064.

25 A. Affeld, G. M. Hühner, C. Seel and C. A. Schalley, Rotaxane or Pseudorotaxane? Effects of Small Structural Variations on the Deslipping Kinetics of Rotaxanes with Stopper Groups of Intermediate Size, *Eur. J. Org. Chem.*, 2001, (No. 15), 2877–2890, DOI: 10.1002/1099-0690(200108)2001:15<2877::AID-EJOC2877>3.0.CO;2-R.

26 P. Linnartz, S. Bitter and C. A. Schalley, Deslipping of Ester Rotaxanes: A Cooperative Interplay of Hydrogen Bonding with Rotational Barriers, *Eur. J. Org. Chem.*, 2003, (No. 24), 4819–4829, DOI: 10.1002/ejoc.200300466.

27 M. A. Soto and M. J. Maclachlan, Disabling Molecular Recognition through Reversible Mechanical Stoppering, *Org. Lett.*, 2019, **21**(6), 1744–1748, DOI: 10.1021/acs.orglett.9b00310.

28 S. Y. Hsueh, C. C. Lai, Y. H. Liu, Y. Wang, S. M. Peng and S. H. Chiu, Protecting a Squaraine Near-IR Dye through Its Incorporation in a Slippage-Derived [2]Rotaxane, *Org. Lett.*, 2007, **9**(22), 4523–4526, DOI: 10.1021/ol702050w.

29 Y. Qiu, Y. Feng, Q. H. Guo, R. D. Astumian and J. F. Stoddart, Pumps through the Ages, *Chem*, 2020, **6**(8), 1952–1977, DOI: 10.1016/j.chempr.2020.07.009.

30 C. Cheng, P. R. McGonigal, S. T. Schneebeli, H. Li, N. A. Vermeulen, C. Ke and J. F. Stoddart, An Artificial Molecular Pump, *Nat. Nanotechnol.*, 2015, **10**(6), 547–553, DOI: 10.1038/nnano.2015.96.

31 Y. Qiu, B. Song, C. Pezzato, D. Shen, W. Liu, L. Zhang, Y. Feng, Q.-H. Guo, K. Cai, W. Li, H. Chen, M. T. Nguyen,

Y. Shi, C. Cheng, R. D. Astumian, X. Li and J. F. Stoddart, A Precise Polyrotaxane Synthesizer, *Science*, 2020, **368**(6496), 1247–1253, DOI: **10.1126/science.abb3962**.

32 T. H. Chiang, C. Y. Tsou, Y. H. Chang, C. C. Lai, R. P. Cheng and S. H. Chiu, Using Slippage to Construct a Prototypical Molecular "Lock & Lock" Box, *Org. Lett.*, 2021, **23**(15), 5787–5792, DOI: **10.1021/acs.orglett.1c01945**.

33 G. Washino, M. A. Soto, S. Wolff and M. J. MacLachlan, Preprogrammed Assembly of Supramolecular Polymer Networks via the Controlled Disassembly of a Metastable Rotaxane, *Commun. Chem.*, 2022, **5**(1), 6–11, DOI: **10.1038/s42004-022-00774-5**.

34 I. T. Harrison, The Effect of Ring Size on Threading Reactions of Macrocycles, *J. Chem. Soc., Chem. Commun.*, 1972, **0**(4), 231–232, DOI: **10.1039/C39720000231**.

35 K. Hirose, K. Ishibashi, Y. Shiba, Y. Doi and Y. Tobe, Control of Rocking Mobility of Rotaxanes by Size Change of Stimulus-Responsive Ring Components, *Chem. Lett.*, 2007, **36**(6), 810–811, DOI: **10.1246/cl.2007.810**.

36 S. Dasgupta and J. Wu, Formation of [2]Rotaxanes by Encircling [20], [21] and [22]Crown Ethers onto the Dibenzylammonium Dumbbell, *Chem. Sci.*, 2012, **3**(2), 425–432, DOI: **10.1039/c1sc00613d**.

37 H. Sugino, H. Kawai, T. Umehara, K. Fujiwara and T. Suzuki, Effects of Axle-Core, Macrocycle, and Side-Station Structures on the Threading and Hydrolysis Processes of Imine-Bridged Rotaxanes, *Chem. – Eur. J.*, 2012, **18**(43), 13722–13732, DOI: **10.1002/chem.201200837**.

38 Y. Tokunaga, T. Iwamoto, S. Nakashima, E. Shoji and R. Nakata, Electrochemical Properties of 3,5-Diphenylaniline Units Encapsulated within a Crown Ether, Effects of the Macrocycle's Aromatic Functionality and Ring Size, *Tetrahedron Lett.*, 2011, **52**(2), 240–243, DOI: **10.1016/j.tetlet.2010.11.043**.

39 K. Zhu, G. Baggi and S. J. Loeb, Ring-through-Ring Molecular Shuttling in a Saturated [3]Rotaxane, *Nat. Chem.*, 2018, **10**(6), 625–630, DOI: **10.1038/s41557-018-0040-9**.

40 M. A. Soto, F. Lelj and M. J. MacLachlan, Programming Permanent and Transient Molecular Protection: Via Mechanical Stoppering, *Chem. Sci.*, 2019, **10**(44), 10422–10427, DOI: **10.1039/c9sc03744f**.

41 M. Naito, T. Fujino, S. Tajima, S. Miyagawa, K. Yoshida, H. Inoue, H. Takagawa, T. Kawasaki and Y. Tokunaga, Ring Size Affects the Kinetic and Thermodynamic Formation of [2]Rotaxanes Featuring an Unsymmetric Bis-Crown Ether Component, *Mater. Chem. Front.*, 2019, **3**(12), 2702–2706, DOI: **10.1039/c9qm00441f**.

42 S. Hoshino, K. Ono and H. Kawai, Ring-Over-Ring Deslipping From Imine-Bridged Heterorotaxanes, *Front. Chem.*, 2022, **10**, 1–10, DOI: **10.3389/fchem.2022.885939**.

43 M. Gaedke, H. Hupatz, F. Witte, S. M. Rupf, C. Douglas, H. V. Schröder, L. Fischer, M. Malischewski, B. Paulus and C. A. Schalley, Sequence-Sorted Redox-Switchable Hetero[3]Rotaxanes, *Org. Chem. Front.*, 2022, **9**(1), 64–74, DOI: **10.1039/d1qo01553b**.

44 H. Y. Zhou, Q. S. Zong, Y. Han and C. F. Chen, Recent Advances in Higher Order Rotaxane Architectures, *Chem. Commun.*, 2020, **56**(69), 9916–9936, DOI: **10.1039/d0cc03057k**.

45 P. R. McGonigal, Multiply Threaded Rotaxanes, *Supramol. Chem.*, 2018, **30**(9), 782–794, DOI: **10.1080/10610278.2018.1433832**.

46 J. J. Danon, D. A. Leigh, P. R. McGonigal, J. W. Ward and J. Wu, Triply Threaded [4]Rotaxanes, *J. Am. Chem. Soc.*, 2016, **138**(38), 12643–12647, DOI: **10.1021/jacs.6b07733**.

47 R. Hayashi, Y. Mutoh, T. Kasama and S. Saito, Synthesis of [3]Rotaxanes by the Combination of Copper-Mediated Coupling Reaction and Metal-Template Approach, *J. Org. Chem.*, 2015, **80**(15), 7536–7546, DOI: **10.1021/acs.joc.5b01120**.

48 L. D. Movsisyan, M. Franz, F. Hampel, A. L. Thompson, R. R. Tykwinski and H. L. Anderson, Polyyne Rotaxanes: Stabilization by Encapsulation, *J. Am. Chem. Soc.*, 2016, **138**(4), 1366–1376, DOI: **10.1021/jacs.5b12049**.

49 J. E. Hertzog, V. J. Maddi, L. F. Hart, B. W. Rawe, P. M. Rauscher, K. M. Herbert, E. P. Bruckner, J. J. de Pablo and S. J. Rowan, Metastable Doubly Threaded [3]Rotaxanes with a Large Macrocycle, *Chem. Sci.*, 2022, 5333–5344, DOI: **10.1039/d2sc01486f**.

50 J. E. M. Lewis, P. D. Beer, S. J. Loeb and S. M. Goldup, Metal Ions in the Synthesis of Interlocked Molecules and Materials, *Chem. Soc. Rev.*, 2017, **46**(9), 2577–2591, DOI: **10.1039/C7CS00199A**.

51 B. M. McKenzie, A. K. Miller, R. J. Wojtecki, J. C. Johnson, K. A. Burke, K. A. Tzeng, P. T. Mather and S. J. Rowan, Improved Synthesis of Functionalized Mesogenic 2,6-Bisbenzimidazolylpyridine Ligands, *Tetrahedron*, 2008, **64**(36), 8488–8495, DOI: **10.1016/j.tet.2008.05.075**.

52 L. A. Wessjohann, E. Ruijter, D. Garcia-Rivera and W. Brandt, What Can a Chemist Learn from Nature's Macrocycles? - A Brief, Conceptual View, *Mol. Divers.*, 2005, **9**(1–3), 171–186, DOI: **10.1007/s11030-005-1314-x**.

53 W. Brandt, V. J. Haupt and L. A. Wessjohann, Chemoinformatic Analysis of Biologically Active Macrocycles, *Curr. Top. Med. Chem.*, 2010, **10**(14), 1361–1379, DOI: **10.2174/156802610792232060**.

54 Q. Wu, P. M. Rauscher, X. Lang, R. J. Wojtecki, J. J. De Pablo, M. J. A. Hore and S. J. Rowan, Poly[n]Catenanes: Synthesis of Molecular Interlocked Chains, *Science*, 2017, **358**(6369), 1434–1439, DOI: **10.1126/science.aap7675**.

55 R. J. Wojtecki, Q. Wu, J. C. Johnson, D. G. Ray, L. S. T. J. Korley and S. J. Rowan, Optimizing the Formation of 2,6-Bis(N-Alkyl-Benzimidazolyl)Pyridine-Containing [3]Catenates through Component Design, *Chem. Sci.*, 2013, **4**(12), 4440–4448, DOI: **10.1039/c3sc52082j**.

56 R. Kramer, J. Lehn, I. L. Bel, U.L Pasteur and A. Marquis-rigault, Self-Recognition in Helicate Self-Assembly: Spontaneous Formation of Helical Metal Complexes from Mixtures of Ligands and Metal Ions, *Proc. Natl. Acad. Sci. U. S. A.*, 1993, **90**, 5394–5398.

57 K. D. Hänni and D. A. Leigh, The Application of CuAAC 'Click' Chemistry to Catenane and Rotaxane Synthesis,

Chem. Soc. Rev., 2010, **39**(4), 1240–1251, DOI: **10.1039/B901974J**.

58 M. Meldal and C. W. Tomøe, Cu-Catalyzed Azide - Alkyne Cycloaddition, *Chem. Rev.*, 2008, **108**(8), 2952–3015, DOI: **10.1021/cr0783479**.

59 M. M. Tranquilli, B. W. Rawe, G. Liu and S. J. Rowan, The Effect of Thread-like Monomer Structure on the Synthesis of Poly[n]Catenanes from Metallosupramolecular Polymers, *Chem. Sci.*, 2023, **14**, 2596–2605, DOI: **10.1039/d2sc05542b**.

60 P. R. Ashton, I. Baxter, M. C. T. Fyfe, F. M. Raymo, N. Spencer, J. F. Stoddart, A. J. P. White and D. J. Williams, Rotaxane or Pseudorotaxane? That Is the Question!, *J. Am. Chem. Soc.*, 1998, **120**(10), 2297–2307, DOI: **10.1021/ja9731276**.

61 G. Schill, *Catenanes, Rotaxanes, and Knots*, Academic Press, New York, 1971.

62 H. Aramoto, M. Osaki, S. Konishi, C. Ueda, Y. Kobayashi, Y. Takashima, A. Harada and H. Yamaguchi, Redox-Responsive Supramolecular Polymeric Networks Having Double-Threaded Inclusion Complexes, *Chem. Sci.*, 2020, **11**(17), 4322–4331, DOI: **10.1039/c9sc05589d**.

63 K. Iijima, D. Aoki, H. Otsuka and T. Takata, Synthesis of Rotaxane Cross-Linked Polymers with Supramolecular Cross-Linkers Based on γ-CD and PTHF Macromonomers: The Effect of the Macromonomer Structure on the Polymer Properties, *Polymer* , 2017, **128**, 392–396, DOI: **10.1016/j.polymer.2017.01.024**.

64 K. Yamamoto, R. Nameki, H. Sogawa and T. Takata, Macrocyclic Dinuclear Palladium Complex as a Novel Doubly Threaded [3]Rotaxane Scaffold and Its Application as a Rotaxane Cross-Linker, *Angew. Chem., Int. Ed.*, 2020, **59**(41), 18023–18028, DOI: **10.1002/anie.202007866**.

65 M. M. Fan, Z. J. Yu, H. Y. Luo, S. Zhang and B. J. Li, Supramolecular Network Based on the Self-Assembly of y-Cyclodextrin with Poly(Ethylene Glycol) and Its Shape Memory Effect, *Macromol. Rapid Commun.*, 2009, **30**(11), 897–903, DOI: **10.1002/marc.200800712**.

66 L. F. Hart, W. R. Lenart, J. E. Hertzog, J. Oh, W. R. Turner, J. M. Dennis and S. J. Rowan, Doubly Threaded Slide-Ring Polycatenane Networks, *J. Am. Chem. Soc.*, 2023, **145**(22), 12315–12323, DOI: **10.1021/jacs.3c02837**.